



HAL
open science

Temporal properties of seismicity and largest earthquakes in SE Carpathians

S. Byrdina, P. Shebalin, C. Narteau, J. L. Le Mouël

► **To cite this version:**

S. Byrdina, P. Shebalin, C. Narteau, J. L. Le Mouël. Temporal properties of seismicity and largest earthquakes in SE Carpathians. *Nonlinear Processes in Geophysics*, 2006, 13 (6), pp.629-639. hal-00331094

HAL Id: hal-00331094

<https://hal.science/hal-00331094>

Submitted on 18 Jun 2008

HAL is a multi-disciplinary open access archive for the deposit and dissemination of scientific research documents, whether they are published or not. The documents may come from teaching and research institutions in France or abroad, or from public or private research centers.

L'archive ouverte pluridisciplinaire **HAL**, est destinée au dépôt et à la diffusion de documents scientifiques de niveau recherche, publiés ou non, émanant des établissements d'enseignement et de recherche français ou étrangers, des laboratoires publics ou privés.

Temporal properties of seismicity and largest earthquakes in SE Carpathians

S. Byrdina¹, P. Shebalin^{1,2}, C. Narteau¹, and J. L. Le Mouél¹

¹Institut de Physique du Globe de Paris, Paris, France

²International Institute of Earthquake Prediction Theory and Mathematical Geophysics Moscow, Russia

Received: 11 August 2006 – Revised: 6 November 2006 – Accepted: 9 November 2006 – Published: 20 November 2006

Abstract. In order to estimate the hazard rate distribution of the largest seismic events in Vrancea, South-Eastern Carpathians, we study temporal properties of historical and instrumental catalogues of seismicity. First, on the basis of Generalized Extreme Value theory we estimate the average return period of the largest events. Then, following Bak et al. (2002) and Corral (2005a), we study scaling properties of recurrence times between earthquakes in appropriate spatial volumes. We come to the conclusion that the seismicity is temporally clustered, and that the distribution of recurrence times is significantly different from a Poisson process even for times largely exceeding corresponding periods of foreshock and aftershock activity. Modeling the recurrence times by a gamma distributed variable, we finally estimate hazard rates with respect to the time elapsed from the last large earthquake.

1 Introduction

Vrancea zone, located at the bend of the Southeast Carpathian arc, is the origin of intermediate-depth lithospheric seismicity. At depth between 80 and 200 km, earthquakes with magnitudes up to M_w 7.8 occur within a small seismogenic body – about 100 km long, 50 km wide. These earthquakes have been responsible for extensive damage to health and property over the last centuries. For example, the strongest events during the twentieth century occurred in 1940 (M_w = 7.7 at a depth d = 160 km), in 1977 (M_w = 7.5, d = 100 km), and in 1986 (M_w = 7.1, d = 135 km). The M_w 7.5 earthquake of 1977 caused damage to some 30 000 apartments, and more than thirty major buildings – most of them in Bucharest, 150 km from the epicenter location (Marza et al., 1991). The crustal seismicity has a larger spatial

distribution, magnitudes M_w < 6, and is separated from the intermediate-depth seismicity by an aseismic layer at a depth between 40 and 60 km.

The African-Eurasian continental collision, which formed the Carpathian mountains, stopped about 10 million years ago (Csontos et al., 1992). Since then, the cooling subduction slab began to steepen and has become almost vertical by now (Hauser et al., 2001). At present, the cold relic slab is denser than the surrounding mantle material and is sinking due to gravity. Ismail-Zadeh et al. (2000) showed with a 2-D numerical model that the combination of buoyancy force and viscous friction produces shear stresses at intermediate depths which may generate the observed confinement of seismicity. In such area, seismic hazard estimation could be better constrained here than in other active fault systems where fault interactions and tectonic motions at larger length scales are likely to add another level of complexity.

The aim of this paper is to study temporal properties of the seismicity in Vrancea. We extend previous studies (e.g. Marza et al., 1991; Mantyniemi et al., 2003; Enescu et al., 2005) by the estimation of the hazard rate distribution of the largest events on the basis of various statistical approaches.

First, we study the general features of seismicity in Vrancea using the ROMPLUS (Onescu et al., 1999) catalogue completed by the CSEM (Centre Sismologique Euro-Méditerranéen) data from 2004 on (<http://www.emsc-csem.org>). This catalogue contains the strongest historical events since 984 AD and becomes homogeneous after 1940 for M_w > 5, and after 1982 for M_w > 3 (Fig. 1). Obviously, larger events are present in the catalogue for a longer time than the smaller ones. We therefore use the concepts of the extreme value theory which allow one to estimate the return levels of extreme events based exclusively on the tail of the distribution – i.e. earthquakes with a magnitude exceeding some predefined threshold. Using this approach, we model the seismicity data by the generalized Pareto distribution (GPD) (Pisarenko and Sornette, 2003, 2004). More specifically, we

Correspondence to: S. Byrdina
(iana@ipgp.jussieu.fr)

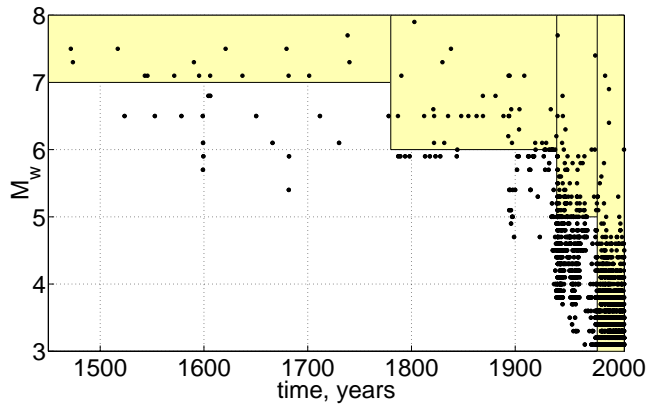


Fig. 1. ROMPLUS seismicity catalogue, 1450–2005 AD. Yellow color marks the homogeneous part of the catalogue which was used for calculations for Figs. 5, 10.

describe the behaviour of the tail of the frequency-magnitude relationship, and we estimate the hazard rate beyond the knee of Gutenberg-Richter's relationship under the assumption that a seismicity rate in the whole Vrancea area, averaged over a long period of time, is constant (e.g. no changes in tectonic setting, like velocities, direction of motion etc.).

The underlying assumption of a time invariant seismicity distribution limits the applicability of the method. If the seismicity is clustered in time, the hazard rate derived from Gutenberg-Richter's law or general Pareto distribution will be over- or underestimated. In Vrancea, time-clustering behavior of large earthquakes is a controversial issue especially looking at the sequence of large earthquakes during the 20th century (4 earthquakes with $M_w \geq 6.9$ between 1940 and 1990) (Purcaru, 1979; Trifu and Radullian, 1991; Enescu and Enescu, 1999). Then the hazard assessment can also use the distribution of recurrence times in order to estimate the evolution of the probability for a large event to occur over long times.

On the one hand, it is often suggested that the recurrence times of the main shocks are distributed exponentially, according to the memoryless Poisson process (e.g. Gardner and Knopoff, 1974); hence the recurrence time of an event does not on the time elapsed from the last event. On the other hand, for some faults the largest earthquakes show some periodicity in their recurrence, while their aftershock areas do not overlap in space (e.g. McCann et al., 1979). These observations, consistent with the assumption of a steady motion of rigid tectonic plates, gave rise to the so called gap theory (Fedotov, 1965; Mogi, 1982; Kagan and Jackson, 1995). The gap theory offered a basis for estimating the recurrence times of strongest earthquakes from the historical catalogues. As was pointed out by Aki (2003): "... the gap theory implies a departure from the Poisson process with the probability of occurrence increasing with the time from the last event while

the earthquake catalog data invariably indicated the departure in the opposite sense, namely, the probability decreasing with the time from the last event (e.g. Aki, 1956)".

In the last decades, much work was dedicated to the modeling of recurrence time distribution; for example, in order to describe the memory of the process, several distributions related to exponential were introduced – Gumbel distribution (Kijko and Sellevoll, 1981), Weibul distribution (Cornell and Winterstein, 1988), gamma distribution (Corral, 2003), stretched exponential (Altmann and Kantz, 2005, and references therein). Bak et al. (2002) found that the distribution of the spatio-temporal occurrence of all events has a scale-free behaviour whatever they are aftershocks, main shocks or foreshocks. Corral (2005a) evidenced a scaling invariance of the hazard rate function; the hazard rate is a time decaying function meaning that the probability for an earthquake to occur decreases – as it was pointed out by Aki (2003) – with increasing waiting time, or in other words, that earthquakes are clustered in time independently on the scale of observation. Immediately after an earthquake there is a high probability of return; then the probability decays with time, and even for long times and large magnitudes, is not properly described by a Poisson process.

An extended recurrence time analysis for earthquakes in the Vrancea area was recently performed by Enescu et al. (2005). These authors used a data catalogue beginning in 1974 and found that, with the exception of aftershock activity, the recurrence times of small and intermediate size events were distributed according to a Poisson process. The unified scaling law of Bak et al. (2002) states however that the statistics of the small and large events are self-similar within a characteristic space range. The results of Enescu et al. (2005) were obtained by averaging the distribution of smaller events over the whole area of observation. The exponential distribution of recurrence times is possibly a consequence of spatial averaging. Even if the local distributions of recurrence times are not exponential in separate volumes, their superposition approaches the poisson process. To avoid this spatial averaging, we observe earthquakes with $M > 4$ and without mixing of the local distributions.

2 Methods

2.1 Generalized Extreme Value (GEV) distribution and Generalized Pareto Distribution (GPD)

In this section, we refer to some elements of extreme value theory (Coles, 2001) that we applied to study the tail of the distribution of the earthquake sizes using only events with magnitude above a predefined threshold. It allows one (1) to fit efficiently the magnitude-frequency distribution in the tail only, and (2) to use an incomplete seismicity catalogue with lesser events missing, but containing reliable magnitudes and times of the largest events. The mathematical basis of this

technique is a limit theorem stating that, under some general conditions, the distribution of a random quantity exceeding some predetermined threshold (excess distribution) can be approximated by the so-called Generalized Pareto distribution (GPD), which depends on two parameters – scale and shape. GPD is closely related to the so called generalized extreme value distribution, and it is convenient to begin with the later.

Let X_1, X_2, \dots, X_n be a sequence X of independent random variables with a common distribution function $F(X)$ and

$$M_n = \max\{X_1, \dots, X_n\} \tag{1}$$

– the maxima for n observation periods of fixed and equal length called block maxima.

For large enough n and in very general conditions, the distribution of the block maxima M_n has the form

$$P\{M_n \leq z\} \approx G(z) = \exp\left\{-1 + \xi \left(\frac{z - \mu}{\tilde{s}}\right)^{-1/\xi}\right\} \tag{2}$$

for some $\mu, \tilde{s} > 0$ and ξ . Interestingly, $G(z)$ does not depend on the original distribution of X .

Furthermore, for values X exceeding some predefined (large enough) threshold u , the distribution function $F_u(x)$ of $(X - u)$,

$$F_u(x) = P\{X - u > x \mid X > u\}, x \geq 0 \tag{3}$$

tends to the Generalized Pareto Distribution (GPD)

$$H(y) = 1 - \left[1 + \xi \frac{y}{s}\right]^{-1/\xi} \tag{4}$$

defined on $\{y_i = X - u > 0, (1 + \xi y/s) > 0\}$. The limit excess distribution $H(y)$ does not depend on the original distribution of X .

The shape parameter $\xi \neq 0$ is the same for GEV distribution and GPD. The scale parameter $s > 0$ is related to the \tilde{s} of GEV distribution by

$$s = \tilde{s} + \xi(u - \mu)$$

Both parameters of GPD, ξ and s can be obtained through a maximum likelihood estimation. While the scale parameter s depends on the threshold value u , the shape parameter ξ , which is dominant in determining the qualitative behaviour of GPD, is independent of it.

An important question is the estimation of the extreme quantiles – i.e. the recurrence probabilities for the largest events $X > u$. Again, suppose that these excess values are modeled by a GPD with parameters ξ and s , then

$$P\{X - u > y \mid X > u\} = [1 + \xi y/s]^{-1/\xi} \tag{5}$$

Letting now $P\{X > x\} = 1/m$, we get the level x_m that is exceeded on average once every m observations by solving

$$\zeta_u \left[1 + \xi \left(\frac{x_m - u}{s}\right)\right]^{-1/\xi} = \frac{1}{m} \tag{6}$$

i.e.:

$$x_m = u + \frac{s}{\xi} [(m\zeta_u)^\xi - 1] \tag{7}$$

where $\zeta_u = P\{X > u\}$. This is valid for m large enough to ensure that $x_m > u$. Usually the return levels plots are given on an annual logarithmic scale, so that, let's say, the 10-year level magnitude is the magnitude $M_{w > x_m}$ expected to be exceeded once every 10 years.

2.2 Recurrence times distribution

In addition to the probability distribution of the extreme events described in the previous section, we also studied the distribution function of the waiting times between earthquakes.

We have calculated the recurrence times density function $D(\tau)$,

$$D(\tau) = \frac{P[\tau < \tau' < \tau + d\tau]}{d\tau}$$

the survivor function – the probability that an earthquake does not occur until time τ ,

$$Z(\tau) = P[\tau' > \tau]$$

and the hazard rate $\lambda(\tau)$ – probability that an earthquake occurs in the time interval $(\tau, \tau + d\tau)$ at τ under the condition that there was no earthquake during the time τ

$$\lambda(\tau) = \frac{P[\tau < \tau' < \tau + d\tau \mid \tau' > \tau]}{d\tau} = \frac{D(\tau)}{Z(\tau)}$$

following Bak et al. (2002) and Corral (2005a).

Bak et al. (2002) divided the whole area of observation onto regions of size $L \times L$ degrees in the north-south and east-west direction and considered groups of earthquakes with magnitude larger than a certain threshold value m_c . For these sets of events they obtained distributions of recurrence times, with a power-law behaviour over short times and a faster (exponential) decay for longer times corresponding to a gamma distribution. The recurrence probability densities for different magnitude thresholds and region sizes collapse onto a single curve if rescaled by R ($\tau \rightarrow \tau R$), where R is the average number of earthquakes with magnitude $M_w > m_c$ in the area $L \times L$ per unit time. Scaling laws for the survival and hazard rate functions, for different m_c and L , were discussed by Corral (2003). This empirical scaling function was shown (Saichev and Sornette, 2006a,b) to be consistent with the ETAS model of earthquake triggering proposed by Ogata (1988). Corral (2005a) suggested a gamma distribution as a model for the recurrence time distribution. This distribution gives a power-law behavior near $t=0$, and exponential one at large times. For a gamma distributed variable, the probability density function $f_\gamma(\tau)$ is given by:

$$f_\gamma(\tau) = \beta^\alpha \frac{\tau^{\alpha-1} \exp(-\beta\tau)}{\Gamma(\alpha)} \tag{8}$$

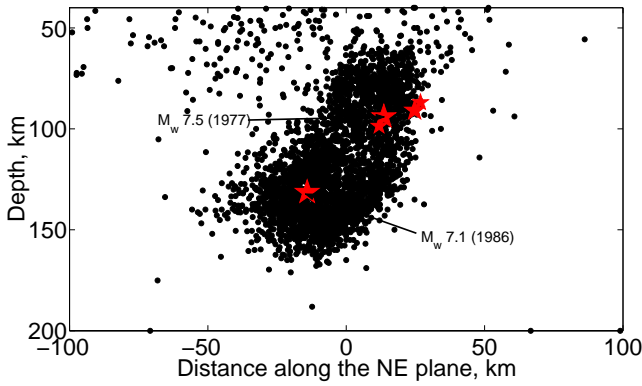


Fig. 2. Projection of the earthquake foci in the NE-SW vertical plane. Red stars indicate the foci of the largest events ($M_w \geq 6.0$) recorded after 1980, and also the focus projection of the M_w 7.5 earthquake occurred in 1977.

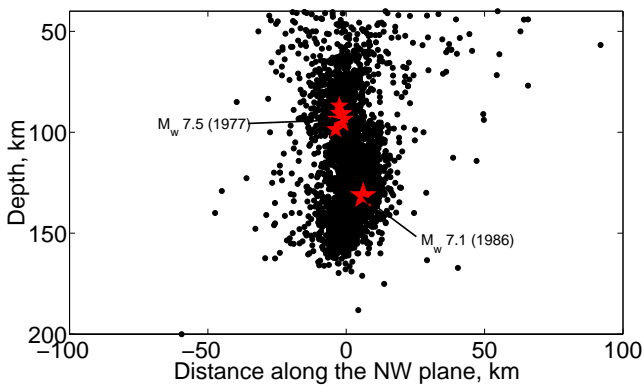


Fig. 3. Projection of the earthquake foci in the NW vertical plane.

where $\alpha > 0$ and $\beta > 0$ are parameters. The cumulative survival function is then

$$Z_\gamma(\tau) = 1 - \frac{\Gamma_{\tau\beta}(\alpha)}{\Gamma(\alpha)}, \quad (9)$$

where $\Gamma_\tau(\alpha) = \int_0^\tau \tau'^{\alpha-1} \exp(-\tau') d\tau'$ is the incomplete Gamma function and the hazard function λ_γ is given by

$$\lambda_\gamma(\tau) = \frac{\tau^{\alpha-1} \exp(-\beta\tau)}{\Gamma(\alpha) - \Gamma_{\tau\beta}(\alpha)} \quad (10)$$

3 Data

The seismicity in Vrancea area is distributed along a NE-SW vertical plane. The projection of the earthquakes foci on this plane is shown in Figs. 2 and 3. In the following, for all calculations which imply information about the spatial distribution of events, we consider data in this projection.

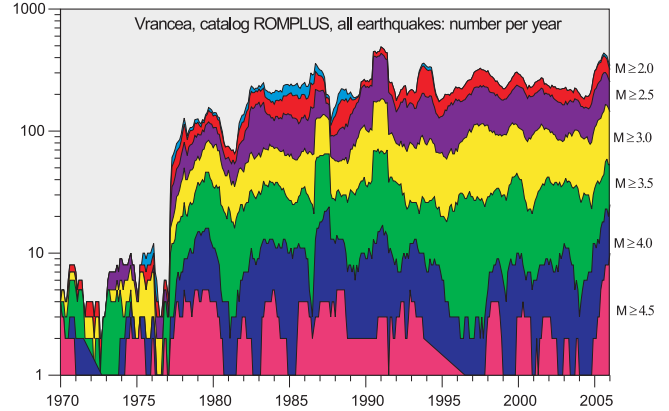


Fig. 4. Number of earthquakes per year. The catalogue is homogeneous since 1982 for events $M_w > 3$. One recognizes aftershocks of the two largest earthquakes since 1980 – M_w 7.1 occurred in 1986 and M_w 6.9 occurred in 1990.

Here and later only events with $M_w > 3$ and depth $d > 40$ km are considered.

The ROMPLUS seismicity catalogue, covering the last ten centuries, contains data of very different quality, as can be seen in Fig. 1 where the data from 1450 AD on are shown (till 1450 there are only records of largest events with a magnitude resolution of 0.5). Figure 4 presents the time dependent form of the Gutenberg-Richter’s law from 1970 on. One can see that the catalogue has become homogeneous for $M_w > 3$ since 1982. This period was used for the statistics of smaller events – with $M_w < 5$. During this time period, two events with $M_w > 6.5$ occurred.

4 Results

4.1 Gutenberg-Richter relationship

The incompleteness of the catalogue for various magnitudes and time intervals makes the calculation of b -value of the GR’s law not straightforward. The b -value estimates in the range $b = 0.65 - 0.78$ have been reported in the literature (see for example Table 2 in Marza et al., 1991). Because of the heterogeneity of the catalogue (Fig. 1), events with $M_w < 5$ were used after 1981, $5 < M_w < 6$ after 1940, events $6 < M_w < 6.5$ after 1780 and $M_w > 6.5$ after 1400. The Gutenberg-Richter’s relationship for these data

$$\log N = 3.98 - 0.78 M_w$$

is shown in Fig. 5.

4.2 Estimation of return levels from GPD model

The results presented in this section have been obtained using the “extRemes”-package of the R-language available under <http://CRAN.R-project.org/>.

Initially, we fitted the GPD model using data from the 1780–2005 interval with magnitudes exceeding $M_w=6$. To obtain regularly sampled data, we took daily maximum values or zeros for days with no data available (we will call it “complete” data set). The maximum likelihood estimates of the model parameters are $\xi=-0.44\pm 0.10$ and $s=0.9\pm 0.1$, based on 49 observed excesses.

Then, we preprocessed the data taking only the block maxima over two years, which allowed us to obtain more homogeneous data records for this period of time (“block maxima” data set, with no missing values). For 56 excesses of the threshold $M_w=5.7$, we obtained values of $\xi=-0.42\pm 0.09$ and $s=1\pm 0.1$. The corresponding GPD fit curve is shown in red in Fig. 5. The results agree well with those of Mantyniemi et al. (2003) obtained by a different method.

The simplest way to estimate the quality of the model is to compare it to the data, using for example probability and quantile plots (Fig. 6). Here the empirical data are compared to the values provided by the GPD model with the estimated parameters. Probability plot consists of the pairs

$$\left\{ \frac{i}{k+1}, H(y_{(i)}); i = 1, \dots, k \right\} \quad (11)$$

for $\xi \neq 0$. Here the H is the GPD discussed in Sect. 2.1, Eq. (4), k – the number of points, and $y_{(i)}$ – the ordered excess data.

Quantile plot consists of the pairs

$$\left\{ H^{-1}\left(\frac{i}{k+1}\right), y_{(i)}; i = 1, \dots, k \right\} \quad (12)$$

If the GPD model is a fair representation of the empirical distribution, both probability and quantile plots are expected to be approximately linear, a condition which is met in our case (Fig. 6).

In Fig. 6, the return level plot, defined in Sect. 2.1 (Eq. 7), is presented inside its 95% confidence interval curves. Using the maximum likelihood method, we estimate a return level magnitude interval of 6.8–7.2 for a return period of 20 years.

As the shape and scale parameters for both the “complete” and the “block” data set based models are close to each other, the return levels (at 95% confidence) are identical – e.g. an event with $M_w=6.9$ (6.8–7.2) is expected every 20 years; an event with magnitude $M_w=7.5$ (7.2–7.8) – every 100 years. Return plots can be obtained alternatively by using the GEV model (Coles, 2001). The algorithm is quite similar, but instead of fitting the threshold excesses to the GPD (Eq. 4) the block maxima are fitted to the GEV distribution (Eq. 3). Because of the catalogue incompleteness before 1900 AD, it was necessary to take 4-year block maxima to obtain convergence of the GEV model. The GEV model then gives a 10 years return level for $M_w=6.4$ (6.1–6.6), in perfect agreement with the GPD model – 6.4 (6.4–6.5), and a 20 years return for level $M_w=6.9$ (6.7–7.2).

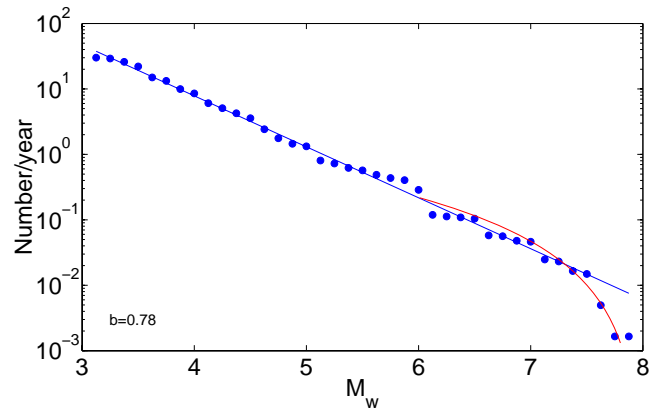


Fig. 5. Gutenberg-Richters relationship (blue line). Complementary cumulative GPD function (red line).

4.3 Recurrence time distribution

The calculation of the recurrence time probability density D is straightforward, and consists in recording the occurrence times t_j of the subsequent earthquakes in regions of size L and the time intervals $\tau_i=t_i-t_{i-1}$ between them. As discussed by Bak et al. (2002), the recurrence time probability function D , for different region sizes L and magnitude cut-offs, scales as L^{d_f}/S^{-b} where S is the seismic moment, d_f is the fractal dimension and b – the slope of GR’s law. The Vrancea seismicity is strongly localized in the horizontal coordinates and distributed close to a vertical plane (Figs. 2 and 3), therefore, to delimit regions (L), it seems reasonable to change only the depth interval, keeping the horizontal dimensions constant. Two different region sizes were used: (1) the whole Vrancea area with depth range $\delta d \approx 150$ km (Fig. 2); (2) a subinterval $135 < d < 200$ km containing aftershock sequence of only one strong earthquake ($M_w=7.1$ in 1986).

First, we compute the maximum likelihood estimates of the parameters α and β of the density function in Eq. (8) for earthquakes with $m_c \geq 5.8$ in the time interval 1780–2005 AD occurred in the whole Vrancea area (red points in Fig. 7a). The blue line represents the best gamma fit $f_\gamma(\tau)$, obtained for $\alpha=0.75$. β -value is assumed to be equal to the average seismic rate $R(L, m_c)$ for corresponding magnitude cutoff: $\beta=R(L, m_c)=0.5$. The earthquake occurrence times t_i are clearly clustered (Fig. 7b).

Now, for a magnitude threshold $m_c=4.2$, we consider the earthquakes located $d > 135$ km. The resulting probability function $D_{(m_c=4.2)}(\tau)$ is presented in Fig. 8a ($\alpha=0.65$, $\beta=R(L, m_c)=2.5$). Occurrence times (Fig. 8b) show similar clustering as in Fig. 7b.

To prove that this evidence of the temporal clustering of earthquakes with $M_w > 4.2$ can not be attributed to the poor quality of the catalogue, we analyze the completeness of the catalogue for this depth interval, following the phasor sum

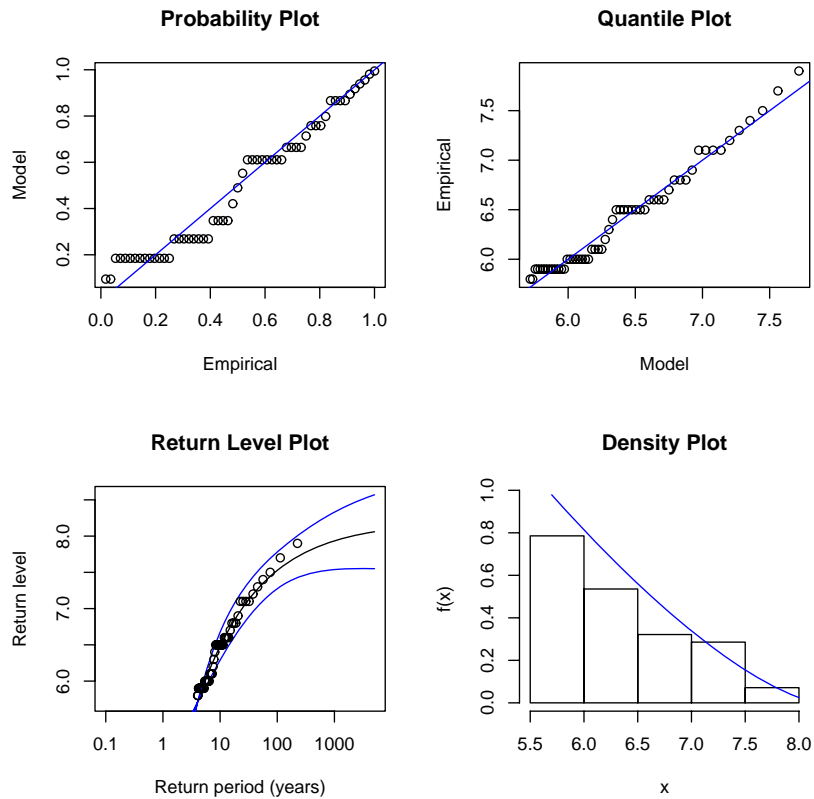


Fig. 6. GPD model diagnostics for a model fitted for 2-year block maxima 1780–2005 A.D., with a threshold of $M_w > 5.7$ inside the 95% confidence interval.

model proposed by Rydelek and Sacks (1989). The phasor sum of $N=72$ earthquakes with magnitudes $M_w > 4.2$ (where we excluded all events occurred during 100 days after the $M_w=7.1$ earthquake in 1986) is compared to the length $l=1.73\sqrt{N}$ given by 95% confidence level of an equivalent random walk. As this radius is not exceeded in our case (Fig. 9), the catalogue can be considered as complete for this magnitudes and depth interval.

Reassured by these two examples of temporal clustering, we will attempt to obtain a more general result. Normalizing waiting times by $R(L, m_c)$ we obtain the scale-free form of $D_{(L, m_c)}(\tau)/R$ for different L and m_c . Estimated from the GR law, R is taken as the average number of earthquakes with a seismic moment exceeding $S=10^{m_c}$ in the region L during the time interval τ . Figure 10a shows the recurrence density $D(\tau)/R$ for two different region sizes and magnitude cutoffs m_c as a function of rescaled dimensionless time $R\tau$. For $m_c=5.5, 6.5$ the whole Vrancea area is considered ($40 < d < 200$ km), for $m_c=4$ earthquakes with depths $135 < d < 200$ km during the same period of time are taken into account.

The red line in Fig. 10a is the density function f_γ calculated from Eq. (8) with an α -value obtained by fitting the events with $M_w \geq 5.8$ after 1780 AD (Fig. 7) and $\beta=R(L, m_c)$.

In Fig. 10a, magenta points show the effect of mixing local distribution functions: here recurrence times are calculated for two different areas ($40 < d < 135$ and $135 < d < 200$ km) and put together to obtain the $D_{(m_c=4, L1-L2)}(\tau)$. The resulting mixed distribution deviates from the analytical curve (red line) over long times, where it approaches another power law (as discussed in detail by (Corral, 2005b)). Thus, the assumption that recurrence times are gamma distributed seems valid for local recurrence time distributions.

Finally, we calculate the hazard rate function $\lambda(\tau)=D(\tau)/Z(\tau)$ following Corral (2005a) (Fig. 10b). In agreement with his results, we obtain a hazard function that decreases with elapsed time, which indicates a temporal clustering of earthquakes. For a Poisson process, $\alpha=1$, the hazard rate is constant in time and equal to the average seismicity rate R .

Another but related measure of temporal clustering is given by the correlation dimension D_2 of recurrence times introduced by Grassberger and Procaccia (1983), which is a special case of generalized fractal dimension D_q for $q=2$ (e.g. Borgani et al., 1993):

$$D_q = \frac{1}{(q-1)} \lim_{r \rightarrow 0} \frac{\log(\sum_{j=1}^{j=N} (P_j(r))^q)}{\log(r)}. \quad (13)$$

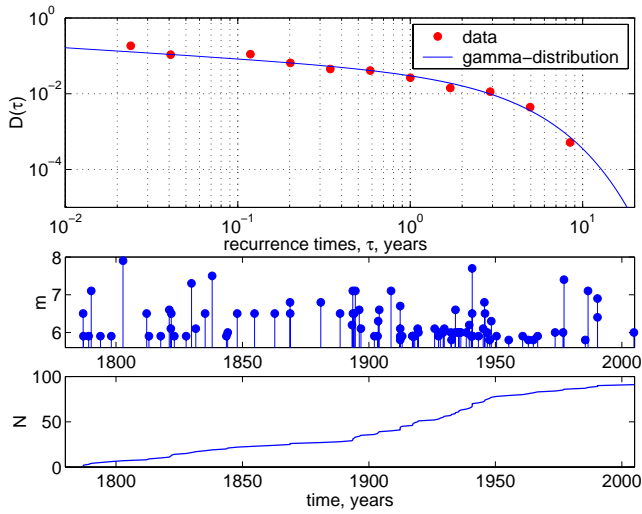


Fig. 7. (a) Gamma fit for recurrence probability $D(\tau)$, earthquakes $M_w \geq 5.8$ since 1780 ($\alpha=0.75$, $\beta=0.5$). (b) Occurrence times of the same events. (c) Accumulated number of the earthquakes shown in the plots (a) and (b). A straight line would correspond to a stationary seismicity with a constant average seismic rate – the slope of the line.

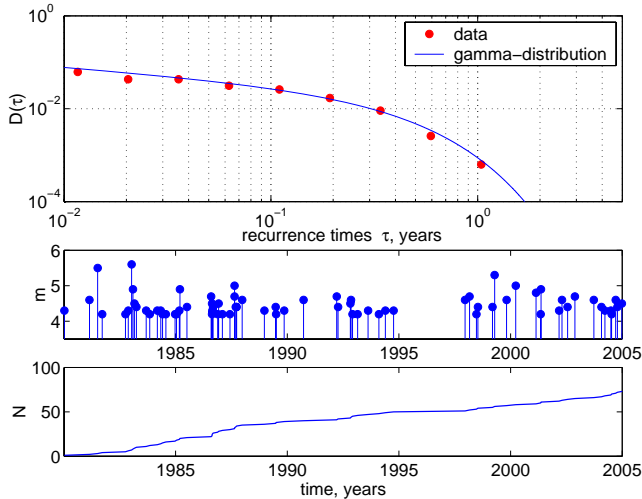


Fig. 8. (a) Gamma fit for recurrence probability $D(\tau)$ to earthquakes $M_w \geq 4.2$ which have occurred at depths $135 < d < 200$ km since 1980 ($\alpha=0.65$, $\beta=2.5$). In this time and depth interval only one earthquake with $M_w > 6$ occurred – the $M_w=7.1$ event in 1986 at depth of 135 km (Fig. 2). One cluster in 1986 corresponds clearly to the aftershock sequence of $M_w=7.1$ event. Aftershocks of $M_w=6.9$ earthquake (depth 90 km) are not seen in this depth interval, but several clusters not related to any strong event can be identified. (b) Recurrence times of the events (c) Accumulated number of the earthquakes shown on the plots (a) and (b).

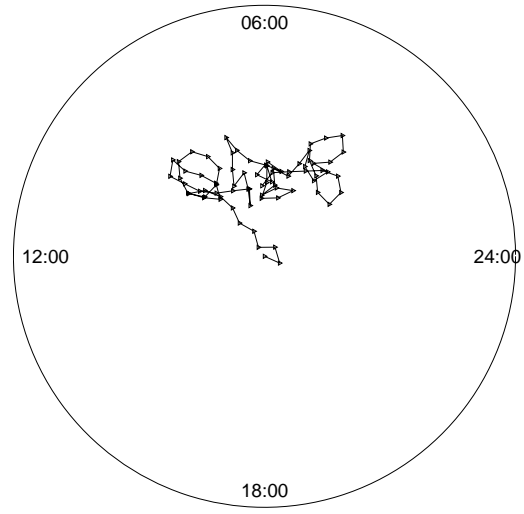


Fig. 9. Phasor sum plots for testing the completeness of 72 earthquakes with $M_w > 4.2$ data on $d > 135$ km depth interval.

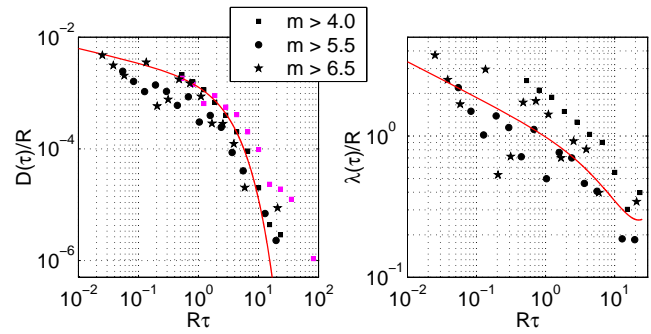


Fig. 10. (a) Probability density distribution function $D_{m_c,L}$ for different sizes L and magnitude cutoffs m_c , rescaled as a function of $(R\tau)$. Here R is the average seismic rate of events with $M_w > m_c$ within a range L . Black color correspond to the local distributions, magenta – to mixed distribution of events (see text). Red line is the probability density function f_γ for a gamma distributed variable with $\alpha=0.75$ (see text). (b) Rescaled hazard rate function $\lambda(\tau)$. The red line shows the λ_γ for a gamma distributed variable.

Here, N is the number of points, the partition function P_j is the probability that the cell j is not empty. P can be defined in different ways. For example, given a finite set of N data points x , P can be related to the correlation function $C_j(r)$ – the fraction of points within a distance r of the j -data point. Then, the partition function P follows

$$P(r, q) = \frac{1}{N} \sum_{j=1}^N C_j(r)^{q-1}. \tag{14}$$

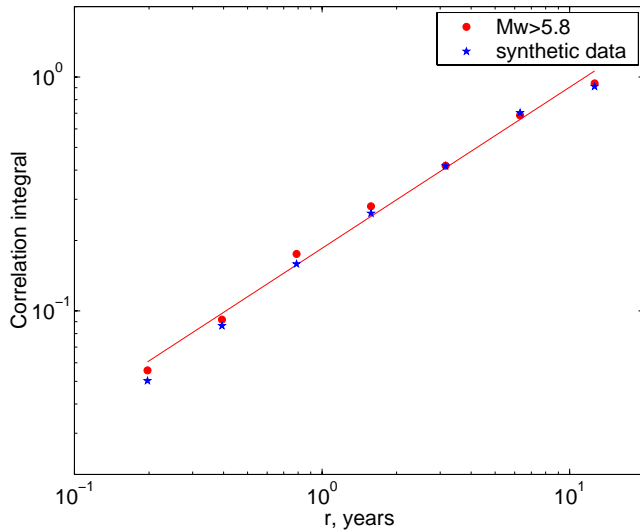


Fig. 11. Fractal dimension estimation for occurrence times of $M_w > 5.8$ events (64 data points since 1780) (circles), with synthetic gamma distributed data with $\alpha=0.75$ and the same number of points (stars). r is box size in years. D_2 is defined by Eq. (15). Straight line gives linear square-root best fit for real data, the slope of the line gives the D_2 value.

If $P(r, q)$ scales as r^d over some range of length-scales, the generalized dimension D_q can be found as

$$d = (q - 1)D_q. \quad (15)$$

For earthquakes with magnitude $M_w \geq 5.8$, we estimated the correlation dimension to be $D_2 = 0.67 \pm 0.06$ (Fig. 11), using the algorithm of unbiased estimation for finite data sets implemented in the R-language (Roberts and Cronin, 1996). The time series for the same time period is shown in Fig. 7b. We estimate the probability to obtain such small value by chance from a Poisson distributed series with the same number of events as less than 5%. For only 47 out of 1000 synthetic Poisson series the D_2 estimation was found to be 0.67 or smaller.

5 Discussion

Figure 10 illustrates the temporal scaling properties of the seismicity in Vrancea. Independently on the magnitude cut-offs and of the nature of the earthquakes – main shocks, aftershocks or foreshocks –, it displays a similar behaviour for all scales. We can use this self similarity to predict the behaviour of the largest events (which we can not study statistically) when we know the statistics of the smaller ones. Assuming that our estimates of average seismicity rates are reliable also for large magnitudes, we thus could predict the recurrence time distribution for events $M_w > 7.5$ based on a fit for events with $M_w \geq 5.8$.

Table 1. Seismic hazard rates for different earthquake magnitudes estimated using Fig. 10b.

		$M_w=5.3 \Leftrightarrow R=1 \text{ yr}^{-1}$		$M_w=7.5 \Leftrightarrow R=0.01 \text{ yr}^{-1}$	
		$\tau \text{ yrs}$	$\lambda \text{ yr}^{-1}$	$\tau \text{ yrs}$	$\lambda \text{ yr}^{-1}$
$R\tau$	0.1	0.1	1.8	10	0.018
	1	1	1	100	0.01
	10	10	0.4	1000	0.004

From the fit of $M_w \geq 5.8$ events after 1780, we obtain $\alpha=0.75$, $\beta=R$ and use these values to estimate the hazard rate as a function of time elapsed after the last earthquake (Fig. 10b). Using this graph, we can read the instantaneous hazard rate (Corral, 2005a). The x-axis represents the dimensionless time $R\tau$, with τ the time elapsed from the last earthquake and R the average seismic rate given by the GR's law or, for large magnitudes, by GPD distribution (Fig. 5). On the y-axis we can read the hazard rate divided by R . Table 1 summarizes some hazard rate estimations obtained from Fig. 10b.

For earthquakes with magnitude $M_w=5.3$ and an averaged rate $R=1$ event/year, the instantaneous hazard rate λ at $\tau=0.1$ years or ≈ 36 days is equal to 1.8 events/year. Thus, the probability of having an earthquake with $M_w > 5.3$ during the 36 days after an event with comparable or greater magnitude is equal to the integral of λ over interval from zero to 0.1: $p = \Gamma_{\tau\beta}(\alpha) / \Gamma(\alpha) \approx 0.19$ (Eq. 9). Such a probability is almost two times higher than the probability obtained from the GR's law. If however the earthquake does not occur till, say, $\tau=10$ years, the hazard rate becomes significantly lower than that predicted by GR's law.

The slope of the hazard rate curve at times $R\tau < 1$ is approximately $\alpha-1$ (Fig. 10b); for a Poisson process the hazard rate does not depend on recurrence time. Obviously, the non-exponential distribution of recurrence times is partly attributed to the aftershock activity (e.g. the cluster observed in 1986 in Fig. 8). On the other hand, the data points in Fig. 10 b evidence decrease of the hazard rate at times extending to $R\tau \approx 1$. This means that the non exponential distribution holds e.g. for earthquakes with magnitude $M_w=7$, $R=0.02 \text{ yr}^{-1}$ for a time period of many years after an earthquake. This time period is significantly longer than the typical duration of the aftershock sequence in Vrancea area, where e.g. after $M_w=6.9$ in 1990 the seismicity returned to the background level after approximately 100 days (Fig. 12). This small number of aftershocks and short duration of the aftershock sequence is typical for intermediate depth earthquakes (Wyss and Toya, 2000). A similar conclusion on the temporal clustering can be drawn from Fig. 11 where the power law behaviour is observed up to several years after the earthquake.

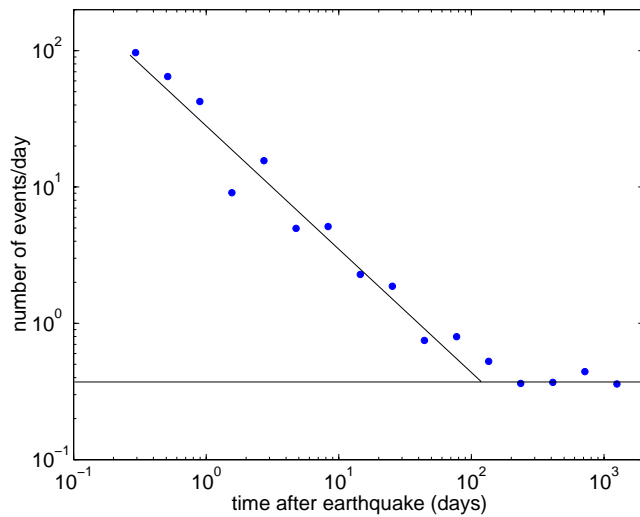


Fig. 12. Decay of the aftershock rate after $M_w=6.9$ earthquake. Seismicity returns to the background seismicity rate approximately 100 days after the main shock.

Enescu et al. (2005), in their multi-fractal study of Vrancea seismicity, came to the conclusion that with exception of the aftershocks, the recurrence times of events $M_w > 2.8$ are distributed according to a Poisson process. These results are complementary to those presented in our study. The exponential distribution of the smaller events can most probably be explained by the fact that in the study of Enescu et al. (2005), the recurrence time distribution was obtained for the whole Vrancea area, thus the local distribution functions were averaged. The spatial averaging can account for the exponential distribution of the resulting recurrence times. If independent local sources generate earthquakes with gamma distributed waiting times, then the resulting superimposed sequence will approach a Poisson process. This is illustrated in Fig. 13. A gamma probability density is shown by blue solid line. First, we generate N gamma distributed sequences of waiting times (with identical parameters $\alpha=0.75$ and $\beta=1/N$). Then we produce N artificial earthquake catalogues calculating occurrence times starting at $t=0$. We obtain the resulting superposition, stacking these catalogues and recalculating the waiting times of the resulting catalogue. As can be seen from Fig. 13, its distribution can be approximated by exponential distribution with $\beta_f=1/\alpha$ (red circles). Therefore, to avoid this spatial averaging, we considered larger events ($M_w > 4$) which have larger source dimensions, and studied their clustering properties in volumes corresponding to the magnitude cutoffs (Bak et al., 2002). For the largest earthquakes, we use the fact that the Vrancea seismic zone is relatively small and isolated from other seismic structures. The largest earthquakes with source volumes comparable to the whole Vrancea area occur practically at the same point, thus, considering only largest events, we avoid the spatial averaging.

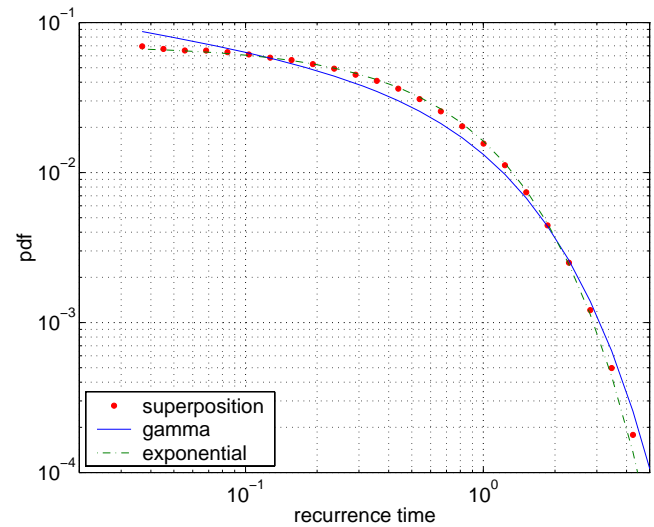


Fig. 13. The solid line represents a gamma probability density function ($\alpha=0.75$). We generate $N=20$ independent earthquake sequences with gamma distributed recurrence times (for each sequence $\alpha=0.75$, $\beta=1/N$). We calculate the occurrence times of events starting at $t=0$ and stack them into a single catalogue. Red dots represent the probability density function of the recurrence times in this catalogue. The dashed line is the best exponential fit of this distribution ($\beta_f=1/\alpha$). This example shows that the superposition of the sequences with gamma-distributed recurrence times approaches a Poisson process.

6 Conclusions

The purpose of this study was to characterize the hazard rate of the largest intermediate-depth earthquakes in Vrancea area, South-Eastern Carpathians.

First, we studied the seismicity rates averaged over the whole period of seismicity records. We then divided the ROMPLUS catalogue into four sub-catalogues, complete for different magnitudes. As the existing results on the Gutenberg-Richter's law for Vrancea area are contradictory (e.g. Marza et al., 1991), we recalculated the frequency-magnitude relationship using these four sub-catalogues for different magnitude cutoffs and obtained $N=3.98-0.78M_w$.

For the earthquakes $M_w > 6$ occurred after 1780 AD, we fitted their magnitude-frequency relationship using the generalized Pareto Distribution model and obtained the return level magnitudes for the expected recurrence times; e.g. for 20 years, $M_w=6.9$ (6.8–7.2 in 95% confidence interval); or, for 100 years, $M_w=7.5$ (7.2–7.8).

As the hazard rate does not depend only on the average seismicity but on the distribution of the recurrence times, we calculated the fractal dimension of the recurrence times and use the approach proposed by Bak et al. (2002) and Corral (2003) to estimate the recurrence time distribution function.

Our fractal dimension estimations ($D_2=0.67$) provide evidence for temporal clustering with a very low probability to be produced by a Poisson process. Therefore, we considered that recurrence times are gamma distributed with $\alpha < 1$, as was proposed by Corral (2003) for clustered data. We calculated the local recurrence time distributions $D(\tau)$ and hazard rate functions λ for magnitude cutoffs $M_w \geq 4, 5.5$ and 6.5 . $\alpha \approx 0.75$ provide the best fit of the distribution function to $M_w \geq 5.8$ events.

This result is in accordance with our D_2 estimation. We produced an artificial sequence of events, by generating inter-occurrence times randomly distributed with probability density given by Eq. (8) with $\alpha=0.75$. Correlation dimension analysis for this sequence (Fig. 11, blue points) gives very similar result. Note that the distribution of recurrence times deviates from exponential even for times largely exceeding the typical duration of the aftershock sequences in the Vrancea area.

The calculated hazard function for all magnitude cutoffs decreases with time, supporting the results from the fractal dimension and giving strong evidence for a temporal clustering of earthquake occurrences. Using the scaling properties of the recurrence time distribution function we predict the hazard rate function for the largest events. The hazard rate function can also be used to improve the risk estimation in the earthquake prediction algorithms.

Acknowledgements. We thank an anonymous reviewer and B. Enescu for their constructive comments. We are grateful to N. Cadichian (Institute of Geodynamics of the Romanian Academy) for providing us with the ROMPLUS catalogue data and M. Ghil for constructive discussions on extreme events. This work was supported by E2C2, a Specific Targeted Research Project of the European Community. In the I.P.G.P., C. Narteau benefited from a Marie Curie reintegration grant 510640-EVOROCK of the European Community. Shebalin was partially supported by Russian Foundation for Basic Researches, project 05-05-64755-a. For analysis of extreme values and fractal dimension the R language and environment for statistical computing has been used (R Foundation for Statistical Computing, Vienna, Austria. ISBN 3-900051-07-0, <http://www.R-project.org>).

Edited by: G. Zoeller

Reviewed by: B. Enescu and another referee

References

Aki, K.: Some problems in statistical seismology, *Zisin (Journal of Seismological Society of Japan)*, 8, 205–207, 1956.
 Aki, K.: Introduction to Seismology for Earthquake Prediction. 29 September–11 October 2003, 7th Workshop on Non-Linear Dynamics and Earthquake Prediction, preprint, 2003.
 Altmann, E. and Kantz, H.: Recurrence time analysis, long term correlations, and extreme events, *Phys. Rev. E*, p. 056106, 2005.
 Bak, P., Christensen, K., Danon, L., and Scanlon, T.: Unified Scaling Law for Earthquakes, *Phys. Rev. Lett.*, 88, 178 501, 2002.

Borgani, S., Murante, G., Provenzale, A., and Valdarnini, R.: Multi-fractal analysis of the galaxy distribution: reliability results from finite data sets, *Phys. Rev. E*, 47, 3879–3888, 1993.
 Coles, S.: An Introduction to Statistical Modeling of Extreme Values, Springer Series in Statistics, London, 2001.
 Cornell, C. and Winterstein, S.: Temporal and magnitude dependence in earthquake recurrence models, *Bull. Seismol. Soc. America*, 78, 1522–1537, 1988.
 Corral, A.: Local distributions and rate fluctuations in a unified scaling law for earthquakes, *Phys. Rev. E*, 68, 035 102, 2003.
 Corral, A.: Time-decreasing hazard and increasing time until the next earthquake, *Phys. Rev. E*, 71, 017 101, 2005a.
 Corral, A.: Mixing of rescaled data and Bayesian inference for earthquake recurrence times, *Nonlin. Processes Geophys.*, 12, 89–100, 2005b.
 Csontos, L., Nagymarosy, A., Horvath, F., and Kovac, M.: Tertiary evolution of the intra-Carpathian area; a model, *Tectonophysics*, 230, 265–276, 1992.
 Enescu, B., Ito, K., Radulian, M., Popescu, E., and Bazacliu, O.: Multifractal and Chaotic Analysis of Vrancea (Romania) Intermediate-depth Earthquakes: Investigation of the Temporal Distribution of Events, *Pure Appl. Geophys.*, 162, 249–271, 2005.
 Enescu, D. and Enescu, B.: Possible cause-effect relationships between Vrancea (Romania) earthquakes and some global geophysical phenomena, *Nat. Hazards*, 19, 233–245, 1999.
 Fedotov, S. A.: Regularities of the distribution of strong earthquakes in Kamchatka, the Kurile Islands, and North-East Japan, *Tr. Inst. Fiz. Zemli Akad. Nauk SSSR*, 36, 66–93, 1965.
 Gardner, J. and Knopoff, L.: Is the sequence of earthquakes in Southern California, with aftershocks removed, Poissonian?, *Bull. Seismol. Soc. America*, 64, 1363–1367, 1974.
 Grassberger, P. and Procaccia, I.: Characterization of Strange Attractors, *Phys. Rev. Lett.*, 50, 346–349, 1983.
 Hauser, F., Raileanu, V., Fielitz, W., Bala, A., Prodehl, C., Polonic, G., and Schulze, A.: VRANCEA99 – the crustal structure beneath the southeastern Carpathians and the Moesian Platform from a seismic refraction profile in Romania, *Tectonophysics*, 340, 233–256, 2001.
 Ismail-Zadeh, A., Panza, G., and Naimark, B.: Stress in the relic slab beneath the Vrancea region, Romania, *Pure Appl. Geophys.*, 157, 11–130, 2000.
 Kagan, Y. and Jackson, D.: New seismic gap hypothesis: five years after, *J. Geophys. Res.*, B, 3943–3959, 1995.
 Kijko, A. and Sellevoll, M.: Triple exponential distribution, a modified model for the occurrence of large earthquakes, *Bull. Seismol. Soc. America*, 71, 2097–2101, 1981.
 Mantyniemi, P., Marza, V., Kijko, A., and Retief, P.: A new probabilistic Seismic Hazard Analysis for the Vrancea (Romania) Seismogenic Zone, *Nat. Hazards*, 29, 371–385, 2003.
 Marza, V., Kijko, A., and Mantyniemi, P.: Estimate of earthquake hazard in the Vrancea (Romania) Seismogenic Region, *Pure Appl. Geophys.*, 136, 143–154, 1991.
 McCann, W., Nishenko, S., Sykes, L., and Krause, J.: Seismic gaps and plate tectonics: Seismic potential for major plate boundaries, *Pure Appl. Geophys.*, 117, 1082–1147, 1979.
 Mogi, K.: Earthquake prediction in Japan, *Science-sha*, 8, 205–207, 1982.

- Ogata, Y.: Statistical models for earthquake occurrences and residual analysis for point processes., *J. Am. Stat. Assn.*, 83, 9–27, 1988.
- Oncescu, M., Marza, V., Rizescu, M., and Popa, M.: The Romanian earthquake catalogue between 984-1997, in: *Vrancea Earthquakes: Tectonics, Hazard and Risk Mitigation.*, edited by: Wenzel, F., pp. 43–47, Kluwer, Dordrecht, 1999.
- Pisarenko, V. F. and Sornette, D.: Characterization of the Frequency of Extreme Earthquake Events by the Generalized Pareto Distribution, *Pure Appl. Geophys.*, 160, 2343–2364, 2003.
- Pisarenko, V. F. and Sornette, D.: Statistical Detection and Characterization of a Deviation from the Gutenberg-Richter Distribution above Magnitude 8., *Pure Appl. Geophys.*, 161, 839–864, 2004.
- Purcaru, G.: The Vrancea, Romania earthquake of March 4, 1977, *Phys. Earth Planet. Int.*, 18, 274–287, 1979.
- Roberts, A. J. and Cronin, A.: Unbiased estimation of multi-fractal dimensions of finite data sets, *Physica A*, 233, 867–878, 1996.
- Rydelek, P. A. and Sacks, I.: Testing the completeness of earthquake catalogues and the hypothesis of self-similarity, *Nature*, 337, 251–253, 1989.
- Saichev, A. and Sornette, D.: “Universal” Distribution of Inter-Earthquake Times Explained, <http://www.citebase.org/abstract?id=oai:arXiv.org:physics/0604018>, 2006a.
- Saichev, A. and Sornette, D.: Theory of Earthquake Recurrence Times, <http://www.citebase.org/abstract?id=oai:arXiv.org:physics/0606001>, 2006b.
- Trifu, C.-I. and Radullian, M.: Frequency magnitude distribution of earthquakes in Vrancea: Relevance for a discrete model, *Bull. Seismol. Soc. America*, 96, 4101–4113, 1991.
- Wyss, M. and Toya, Y.: Is background seismicity produced at a stationary Poissonian rate?, *Bull. Seismol. Soc. America*, 90, 1174–1187, 2000.